Journal Homepage: http://ijcpe.uobaghdad.edu.iq
Iraqi Journal of Chemical and Petroleum Engineering
Vol. 26 No. 1 (March 2025) 67 – 76
EISSN: 2618-0707, PISSN: 1997-4884

Determination of controlling fouling mechanism using the Hermia models and estimation of the manufacturing costs of the modified polyvinylidene fluoride-based ultrafiltration membranes

Abdullah G. Saleem [a], Sama M. Al-Jubouri [b, *], Sirhan Al-Batty [c], Mohammed Wali Hakami [c]

a Department of Chemical and Petrochemical Engineering, College of Engineering, University of Anbar, Anbar, Iraq
b Department of Chemical Engineering, College of Engineering, University of Baghdad, Baghdad, Iraq
c Department of Chemical Engineering, Jubail Industrial College, Jubail, Saudi Arabia

Abstract

Membrane fouling is the main problem that limits the use of membrane technology. This work focuses on using the Hermia models to determine the controlling fouling mechanisms, including intermediate pore blocking, complete pore blocking, standard pore blocking, and cake formation. Also, it investigates the estimation of the manufacturing costs, which included the costs of preparation materials and energy consumed during the preparation and casting processes of the polyvinylidene fluoride/polyethylene glycol (PVDF/PEG) and PVDF/PEG-tin oxide nanoparticles (PVDF/PEG-SnO_2 NPs) membranes. The results of Hermia's models were applied on the first, third, and fifth cycles of the rhodamine B dye solution filtration processes. Depending on linear fitting parameters, the membrane fouling occurred in all fouling mechanism types simultaneously. However, the predominating fouling mechanism was cake formation followed by intermediate pore blocking. Analysis of the parameters of the fouling models validated that the irreversible fouling exceeded the reversible fouling when the correlation factor (R^2) value was higher than 0.95, which explains the continuous reduction of the permeate flux for both studied membranes. The estimated cost of the locally manufactured PVDF-based membranes did not surpass 80 $/m^2 of the membrane. Also, the locally fabricated flat sheet ultrafiltration membranes are cheaper than other pristine PVDF membranes manufactured by Guochukeji Technology (Xiamen) Company.

Keywords: PVDF membrane; PEG, Tin oxide (SnO_2); Fouling mechanisms; Hermia models; Economic estimation.

Received on 06/01/2025, Received in Revised Form on 22/02/2025, Accepted on 22/02/2025, Published on 30/03/2025

https://doi.org/10.31699/IJCPE.2025.1.7

1- Introduction

Water pollution is the biggest environmental challenge facing the world. It severely affects human health, aquatic life, and ecosystems. Water pollution is caused when freshwater resources like rivers, lakes, and groundwater are contaminated with harmful substances like chemicals, sewage, industrial effluents, and pesticides [1, 2]. Water pollution by dyes is a serious environmental issue, particularly in paper, plastic, and textile industries. Synthetic dyes contain harmful chemicals that are difficult to biodegrade. Besides, some colors contain cancer-causing chemicals which can harm human health when contaminating drinking water [3, 4]. Several methods can be used to treat dye pollution including adsorption, membrane filtration, ion exchange, coagulation-flocculation, advanced oxidation, and biological degradation. Water pollution reduction and water quality improvement help to maintain public health, marine life diversity, and water resources, and promote environmental protection [5- 7].

Membrane technology attracts a lot of attention in the effluent processing of a wide range of applications such as food, pharmaceutical, municipal, and industrial wastewater treatment. However, membrane fouling is the major problem facing membrane technology [8- 10]. Membrane separation technologies are expanding in practice to be more economical, efficient, and sustainable [11]. The difficult design and manufacture processes of membranes reflect on their cost. Membrane materials, types, production scales, and applications all have a significant influence on cost [12, 13]. The viability and applicability of membrane-based systems in various sectors like water treatment, gas separation, and biological processing are significantly impacted by the membrane cost [14]. Developing membrane markets and applications demands the development of affordable fabrication processes [15].

Polymeric (organic) membranes have garnered an important industrial concern because of their cost-effectiveness and ease of production [16, 17]. In practical applications, polymeric membranes are widely used compared with inorganic membranes [9]. Membrane fouling is defined as adhering or accumulation of organic, inorganic, or biological foulants on the membrane

*Corresponding Author: Email: sama.al-jubouri@coeng.uobaghdad.edu.iq

surface, which negatively influences the lifetime and performance of the membrane and increases the operation costs [17- 19]. Polymeric membranes are susceptible to fouling after long use due to adsorption and accumulation of organic foulants [20, 21]. The preparation of membranes with high antifouling properties has become an essential goal in the membrane's science [8]. The membrane fouling is governed by hydrophilicity, surface charge, porosity, pores size, roughness, feed concentration, and operation conditions [22].

Hydrophilic membranes offer high resistance to the adsorption of foulants because the hydrophilic surface provides a protective hydration layer that protects the membrane surface from adsorbing foulants. High hydrophilic properties can be achieved by modification with water-soluble polymers i.e., polyethylene glycol (PEG) and polyvinylpyrrolidone (PVP) which act as a pore former and the addition of hydrophilic agents such as inorganic nanomaterials [8, 20]. Mixed matrix membranes (MMMs) have brought higher consideration than pure polymeric membranes because they can improve the adsorption of water on the surface, which minimizes fouling and enhances permeation [17]. Membrane fouling can be either reversible or irreversible. Reversible fouling can be easily removed by washing because the foulants are infirmly bound to the membrane surface. The irreversible fouling cannot be eliminated because foulants are strongly bound to the surface of the membranes or pores [17, 23, 24].

The membrane fouling can occur in four mechanisms as shown in Fig. 1, which are partial (intermediate) pore blocking, complete pore blocking, pore constriction or standard pore blocking, and cake formation [25, 26]. If the foulant particles are larger than the pores, intermediate pore blocking happens when some foulant particles block the pores and other particles deposit on the surface. Complete blocking occurs when particles totally block the pores. When the foulant particles are smaller than the pores, they penetrate through the pores, cover the walls, and cause pore constriction, which is known as standard pore blocking. Cake formation is the most complicated type of fouling and happens when foulant particles are larger than the pores, so they accumulate on the surface to form a cake layer [17].

This study aims to apply the Hermia models to the removal results of rhodamine B (RhB) dye-containing solutions by PVDF/PEG and PVDF/PEG-SnO_2 flat sheet ultrafiltration (UF) membranes to determine the fouling mechanism controlling the filtration process. It also aims to estimate the manufacturing costs of the previously prepared membranes. Cost considerations included evaluating the cost of materials used in preparation and the cost of energy consumed during the preparation of the polymeric solution and casting process.

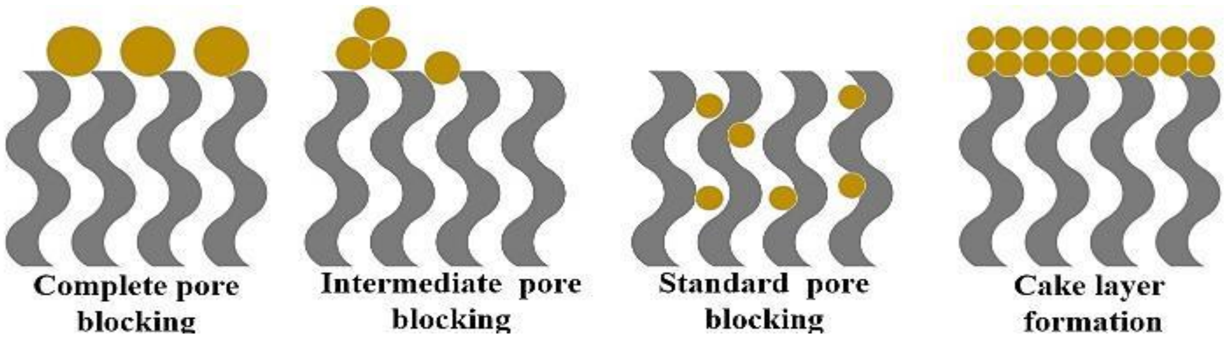

Fig. 1. The membrane fouling mechanisms [27]

2- Experimental work

The membranes chosen for this study were prepared in previous work [2, 28] according to the compositions presented in Table 1 by the phase inversion process. The pure water flux (J_o) and permeate flux (J_p) were studied using a membrane cell that operates in a crossflow system as described in previous work [2]. All experiments were run at room temperature, collection time of 90 min, feed rate of 1 L/min, and transmembrane pressure of 1 bar. Eq. 1 was used to compute the pure water flux and the permeate flux of the polluted solutions containing 10 mg/L of RhB dye.

$$J = \frac{V}{A \times t} \qquad (1)$$

Where J is the flux of pure water and/or permeate ($L/m^2.min$), V is the volume of water permeation (L), A is the effective area of the membrane (m^2), and t is the collection time of permeated water (min). The procedures for membrane reuse were done by cleaning the membranes with distilled water for 10 min after each cycle to be ready for the later run. The antifouling analysis of the PM-2 and PM-3 membranes was evaluated using RhB dye as a model foulant in terms of flux recovery ratio (FRR), reversible fouling ratio (R_r), irreversible fouling ratio (R_{ir}), and total fouling ratio (R_t) as mentioned in previous work [28].

Table 1. The compositions of the materials used in the preparation of membranes

Material	PM-2 membrane (wt%)	PM-3 membrane (wt%)
Polyvinylidene fluoride (PVDF)	18	18
Polyethylene glycol (PEG)	6	6
Tin oxide nanoparticles (SnO_2 NPs)	0	0.3
N, N-dimethyl formamide (DMF)	76	75.7

3- Hermia models

The mechanism of fouling formation on the surface and within the pores of the prepared membranes was analyzed by estimating the filtration resistance acquired through treating the RhB dye-containing wastewater at constant transmembrane pressure. The decline of the membrane flux with time was described using various models. The fouling mechanism in the filtration process of this study was explained using Hermia's model. Hermia developed a general equation which can be used for all types of fouling depending on the value of n as shown in Eq. 2 [27, 29].

$$\frac{d^2t}{dV^2} = K\left(\frac{dt}{dV}\right)^n \tag{2}$$

In a crossflow system, the type of fouling depends on the magnitude of (n) presented in Eq. 2. For partial pore blocking, n = 1. For complete pore blocking, n = 2. For standard pore blocking, n = 3/2. For cake formation, n = 0. The integrated forms of Eq. 2 conducted based on n value are shown in Eqs. 3 - 6 in Table 2 [27, 29].

Table 2. Equations of the membrane fouling mechanisms using Hermia models [27, 30, 31]

Fouling mechanism	Model		Characteristic parameter (unit)
Intermediate pore blocking	$\frac{1}{J_p} = K_i t + \frac{1}{J_o}$	(3)	K_i (m^2/L)
Complete pore blocking	$\ln\left(\frac{1}{J_p}\right) = K_B t + \ln\left(\frac{1}{J_o}\right)$	(4)	K_B (m^2/L)
Standard pore blocking	$\frac{1}{J_p{}^{0.5}} = K_s t + \frac{1}{J_0^{0.5}}$	(5)	K_s ($m/L^{0.5}.min^{0.5}$)
Cake formation	$\frac{1}{J_p{}^2} = K_C t + \frac{1}{J_0^2}$	(6)	K_c ($m^4.min/L^2$)

All models' equations present in Table 2 are a linear relationship between permeate flux and time. The model that has the highest R^2 value indicates the controlling fouling mechanism. The slope of these linear equations, which are K_i, K_B, K_s, and K_c represents the coefficient of intermediate pore blocking, complete pore blocking, standard pore blocking, and cake formation, respectively.

4- Estimation of the membrane manufacturing cost

The total manufacturing cost of the PM-2 and PM-3 membranes was estimated according to Eqs. 7 and 8 considering that the official price of power in Iraq for the government institutions is 120 IQD/kWh which is equivalent to 0.09091 $/kWh. Also, the price of the materials used in the membrane fabrication were set as sold in the local stores.

$$C_t = C_m + C_p \tag{7}$$

$$C_p = P_i * C_{op} \tag{8}$$

Where C_t is the total manufacturing cost ($), C_m is the total cost of materials ($), C_p is the total cost of consumed electrical power ($), P_i is the power of instruments used in the manufacturing of the membrane (kWh), and C_{op} is the official price of power ($/kWh). The total cost of the consumed electrical power includes the power which is consumed in the polymeric solution preparation processes (sonication, drying, and stirring) and the membrane fabrication process (casting process) according to the periods for each process as mentioned in previous works [2, 28].

5- Results and discussion

5.1. Analysis of the membrane fouling mechanisms

The data obtained from the reuse of the PM-2 and PM-3 membranes have been used to determine the controlling fouling mechanism based on Hermia's models. Fig. 2, Fig. 3, and Fig. 4 show the plot of Hermia models of the PM-2 and PM-3 membranes for the first, third, and fifth cycles, respectively. Table 3 revealed the fitting parameters of the first, third, and fifth cycles of the PM-2 and PM-3 membranes. Depending on the R^2 value present in Table 3 and the results of the contact angle test and FRR% reported by Saleem and Al-Jubouri [28], the PM-3 membrane was less prone to dye molecules accumulating after using the membrane for one cycle than the PM-2 membrane. This was because the formation of a hydration layer on the PM-3 membrane surface with a low contact angle inhibited the retention of the dye molecules. Therefore, during the washing process with distilled water, the PM-3 membrane's surface gave a lot of accumulated dye molecules because it has a lower contact angle than the PM-2 membrane.

The results of fitting parameters belonging to the PM-2 membrane show that the R^2 values rose significantly from just above 0.78 to just above 0.96 starting from the third cycle for all models studied. These results validate the results presented in the previous work [28] which reported increasing the R_{ir} above the R_r. Since the cake formation and intermediate pore blocking mechanisms predominant the fouling by the dye in the PM-2 membrane. Outstandingly, the fitting parameters belonging to the PM-3 membrane show that the R^2 values significantly raised in the fifth cycle to be just over 0.97 for all studied fouling models, which came harmonious with the outcomes of the previous work [28] that reported occurring irreversible fouling in the fifth cycle and surpassed the reversible fouling. The linear plots of the complete pore blocking mechanism, which is indicated by the symbol b in Fig. 2, Fig. 3, and Fig. 4 belong to the PM-3 membrane revealed that the intercept with y-axis values is placed within the negative range of the axis. The reason behind this behavior is the improvement of the PM-3 membrane structure properties as a result of incorporating the PEG and SnO_2 NPs which increased the permeate flux significantly. Also, Table 3 shows the predomination of the cake formation followed by the intermediate pore blocking.

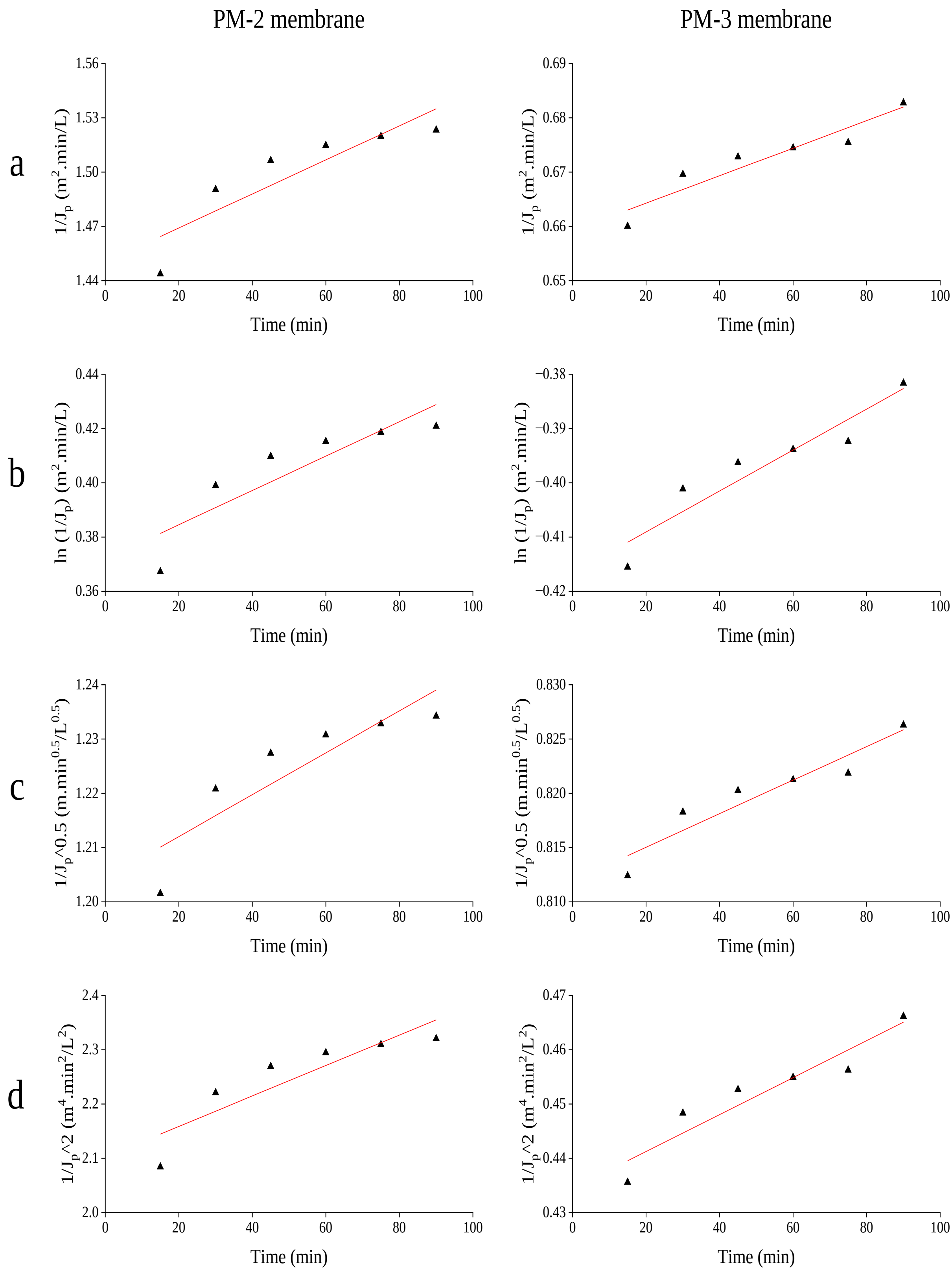

Fig. 2. The linear plots of the fouling mechanism model for the first cycle of the PM-2 and PM-3 membranes. a) intermediate pore blocking, b) complete pore blocking, c) standard pore blocking, and d) cake formation

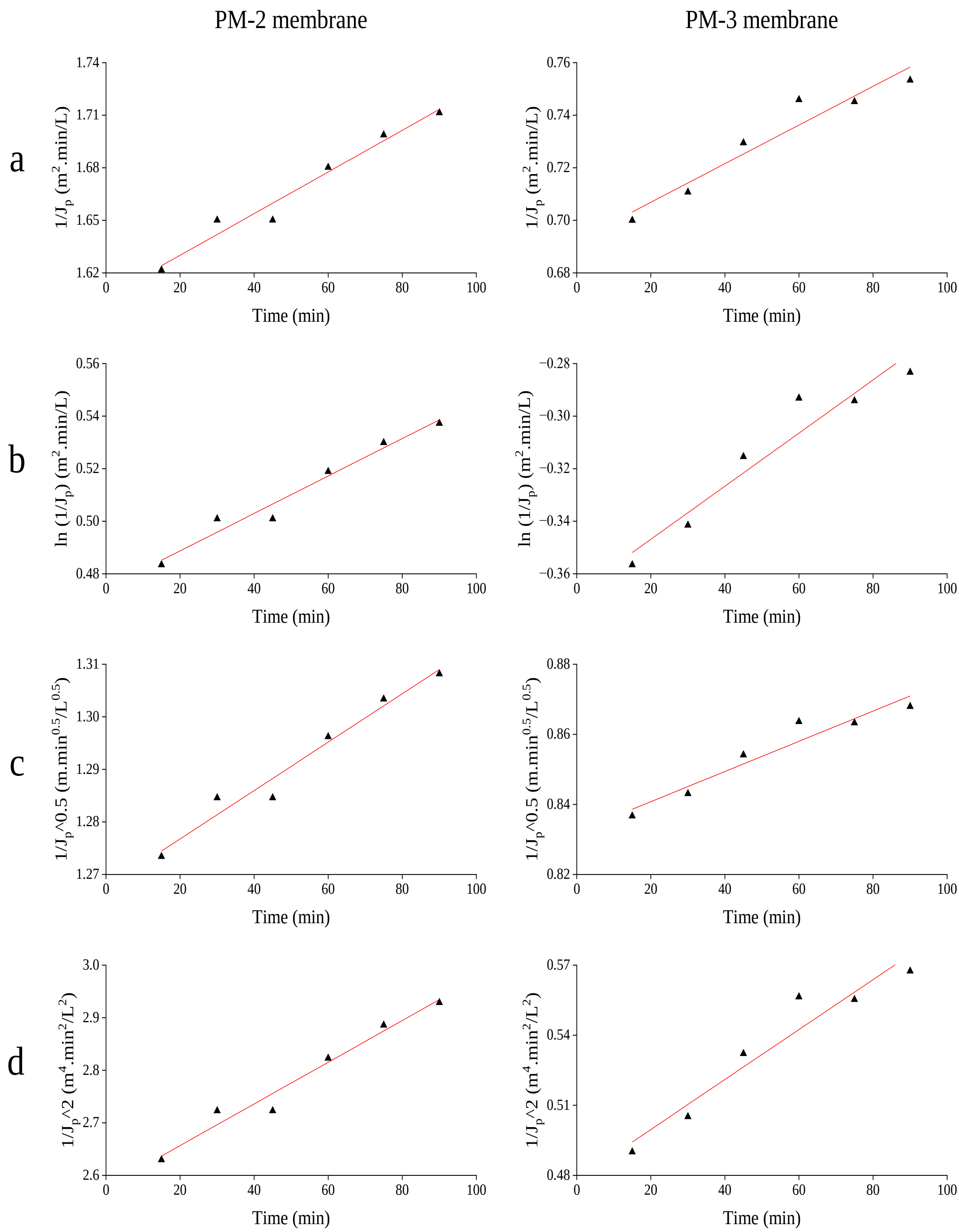

Fig. 3. The linear plots of the fouling mechanism model for the third cycle of the PM-2 and PM-3 membranes. a) intermediate pore blocking, b) complete pore blocking, c) standard pore blocking, and d) cake formation

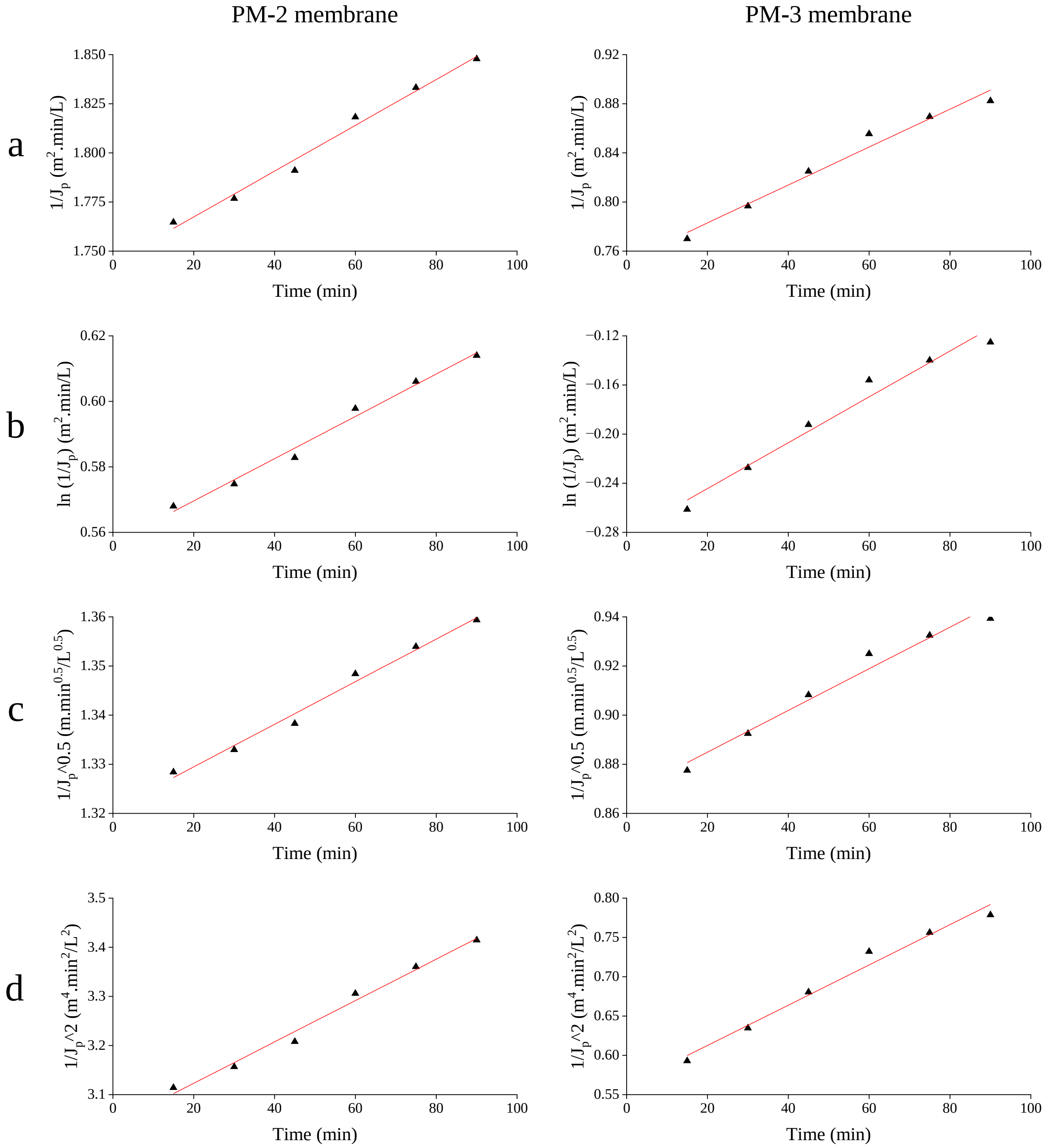

Fig. 4. The linear plots of the fouling mechanism model for the fifth cycle of the PM-2 and PM-3 membranes. a) intermediate pore blocking, b) complete pore blocking, c) standard pore blocking, and d) cake formation

Table 3. Fitting parameters of the first, third, and fifth cycles of the PM-2 and PM-3 membranes

		Intermediate pore blocking	Complete pore blocking	Standard pore blocking	Cake formation
PM-2 membrane	First	R^2 = 0.7841	R^2 = 0.7788	R^2 = 0.7815	R^2 = 0.7895
	cycle	y = 0.0009x + 1.4503	y = 0.0006x + 0.3719	y = 0.0004x + 1.2043	y = 0.0028x + 2.1027
	Third	R^2 = 0.9674	R^2 = 0.9668	R^2 = 0.9671	R^2 = 0.9680
	cycle	y = 0.0012x + 1.6063	y = 0.0007x + 0.4744	y = 0.0005x + 1.2676	y = 0.004x + 2.5772
	Fifth	R^2 = 0.9877	R^2 = 0.9872	R^2 = 0.9874	R^2 = 0.9878
	cycle	y = 0.0012x + 1.7441	y = 0.0006x + 0.5567	y = 0.0004x + 1.3208	y = 0.0042x + 3.0388
PM-3 membrane	First	R^2 = 0.8950	R^2 = 0.8934	R^2 = 0.8942	R^2 = 0.8966
	cycle	y = 0.0003x + 0.6592	y = 0.0004x - 0.4166	y = 0.0002x + 0.8119	y = 0.0003x + 0.4344
	Third	R^2 = 0.929	R^2 = 0.9267	R^2 = 0.9279	R^2 = 0.9312
	cycle	y = 0.0007x + 0.6922	y = 0.001x - 0.3671	y = 0.0004x + 0.8321	y = 0.0011x + 0.4782
	Fifth	R^2 = 0.9753	R^2 = 0.9709	R^2 = 0.9732	R^2 = 0.9792
	cycle	y = 0.0015x + 0.7521	y = 0.0019x - 0.2817	y = 0.0008x + 0.8679	y = 0.0026x + 0.5614

The four studied fouling models revealed good linear fitting during the UF processes of the RhB dye-containing wastewater. This behavior indicates that all types of fouling mechanisms occurred simultaneously. For both membranes, after each washing process, some of the dye molecules cannot be removed physically because they are firmly bound to the surface or pores of the membrane. Particles remaining after each cycle caused a decline in the permeate flux and reduced the difference between one reading and another. Therefore, it was observed that the value of R^2 increased after each cleaning process for both membranes. The above results showed that the dye fouled the membrane fundamentally by forming a cake layer, while a few dye molecules were adsorbed, adhered to the surface, and penetrated through the membrane. Therefore, the permeate flux declined after every time the membranes were reused in the filtration processes. The behavior of these results was consistent with Sadek et al. [27] findings, although the flux was not reduced considerably since the researchers employed chemical cleaning to remove the contaminating molecules that stick to the membrane surface.

5.2. Estimation of the membrane manufacturing costs

The estimation of manufacturing costs has been made per 20 g of the casting solution for the PM-2 and PM-3 membranes according to the ratios shown in Table 1. This dose of a casting solution forms 0.1125 m^2 during casting by the casting machine (film applicator). Table 4 presents details of the material prices used in manufacturing the membranes. It shows that the total cost of the materials used in the manufacturing of the PM-2 and PM-3 membranes were about 6.6592 $ and 6.93478 $, respectively. The total costs of consumed electrical power were 2.08 $ and 2.12 $, while the total manufacturing costs were 8.74 $ and 9.06 $ for the PM-2 and PM-3 membranes, respectively. Table 5 presents a comparison made among the manufacturing prices of the PM-2 and PM-3 membranes and other pristine PVDF flat sheet UF membranes manufactured by Guochukeji Technology (Xiamen) Co., Ltd (China). As advertised by this company, the ex-price of these specified membranes is 180 $/$m^2$, but without the shipping cost. The shipping cost to Iraq is 100 $ by FedEx. So, the total price after shipping to Iraq becomes 280 $. The local manufacturing costs of the PM-2 and PM-3 membranes did not surpass 80 $/$m^2$ per membrane.

Table 4. Prices of materials used in the manufacturing of the PM-2 and PM-3 membranes

Material	Price of the material in the local store ($/g)	Price of the used quantities ($)	
		PM-2 membrane	PM-3 membrane
PVDF	1.515	5.454	5.454
DMF	0.074	1.1248	1.12036
PEG	0.067	0.0804	0.0804
SnO_2 NPs	4.667	0	0.28002
Total cost of the materials		6.66	6.94
Total cost of consumed electrical power		2.08	2.12
Total cost of the membrane manufacturing		8.74	9.06

Table 5. Prices comparison of the locally manufactured membranes with other membranes

Membrane	Filtration accuracy (Da)	Pure water flux (LMH)	Testing conditions	Price ($/$m^2$)	Reference
PM-2	478	75	1 bar 25 °C	78	Current study
PM-3	520	135	1 bar 25 °C	80	Current study
PVDF	250	400 as expected	3.5 bar 25 °C	180	http://www.guochukeji.com/en/
PVDF	500	400 as expected	3.5 bar 25 °C	180	http://www.guochukeji.com/en/

6- Conclusion

In this work, the fouling mechanisms of the PVDF-based UF membranes were successfully studied using Hermia's models. Also, the manufacturing costs of these membranes have been estimated. The results of Hermia's models applied on the first, third, and fifth cycles of the filtration of RhB dye solution showed that the membrane fouling had occurred simultaneously in all fouling mechanism models (intermediate pore blocking, complete pore blocking, standard pore blocking, and cake formation). When the R^2 value of both membranes is higher than 0.95, it indicates that the irreversible fouling exceeded the reversible fouling, which refers to the predominating fouling mechanisms as the cake formation followed by the intermediate pore blocking. Therefore, the permeate flux reduced continuously for both membranes during the filtration time. The estimation of the manufacturing cost revealed that the developed PVDF-based flat sheet UF membranes are cheaper than other pristine PVDF membranes manufactured by Guochukeji Technology (Xiamen) Company.

References

[1] A. S. Adday and S. M. Al-Jubouri, "Photocatalytic oxidative removal of the organic pollutant from wastewater using recyclable Ag2O@CRA heterojunction photocatalyst," *Case Studies in Chemical and Environmental Engineering*, vol. 10, Dec. 2024, https://doi.org/10.1016/j.cscee.2024.100852

[2] A. G. Saleem and S. M. Al-Jubouri, "Separation performance of cationic and anionic dyes from water using polyvinylidene fluoride-based ultrafiltration membrane incorporating polyethylene glycol," *Desalination and Water Treatment*, vol. 319, Jul. 2024, https://doi.org/10.1016/j.dwt.2024.100546

[3] S. Yadav, K. S. Tiwari, C. Gupta, M. K. Tiwari, A. Khan, and S. P. Sonkar, "A brief review on natural dyes, pigments: Recent advances and future perspectives," *Results in Chemistry*, Jan. 01, 2023, Elsevier B.V. https://doi.org/10.1016/j.rechem.2022.100733

[4] Nachiyar V. C., A. D. Rakshi, S. Sandhya, N. Britlin Deva Jebasta, and J. Nellore, "Developments in treatment technologies of dye-containing effluent: A review," *Case Studies in Chemical and Environmental Engineering*, vol. 7, Jun. 2023, https://doi.org/10.1016/j.cscee.2023.100339

[5] A. E. Abdelhamid, A. E. Elsayed, M. Naguib, and E. A. Ali, "Effective Dye Removal by Acrylic-Based Membrane Constructed from Textile Fibers Waste," *Fibers and Polymers*, Jun. 2023, https://doi.org/10.1007/s12221-023-00247-z

[6] A. A. E. A. Elfiky, M. F. Mubarak, M. Keshawy, I. E. T. El Sayed, and T. A. Moghny, "Novel nanofiltration membrane modified by metal oxide nanocomposite for dyes removal from wastewater," *Environment, Development and Sustainability*, 2024, https://doi.org/10.1007/s10668-023-03444-1

[7] H. M. Solayman, M. A. Hossen, A. A. Aziz, N. Y. Yahya, K. H. Leong, L. C. Sim, M. U. Monir , and K. D. Zoh, "Performance evaluation of dye wastewater treatment technologies: A review," *Journal of Environmental Chemical Engineering*, Jun. 01, 2023, Elsevier Ltd. https://doi.org/10.1016/j.jece.2023.109610

[8] D. Liu, T. Wang, and C. He, "Antifouling polyethersulfone membrane blended with a dual-mode amphiphilic copolymer," *Journal of Materials Science*, vol. 51, no. 16, pp. 7383–7394, Aug. 2016, https://doi.org/10.1007/s10853-016-9904-9

[9] B. Khorshidi, S. A. Hosseini, G. Ma, M. McGregor, and M. Sadrzadeh, "Novel nanocomposite polyethersulfone- antimony tin oxide membrane with enhanced thermal, electrical and antifouling properties," *Polymer*, vol. 163, pp. 48–56, Feb. 2019, https://doi.org/10.1016/j.polymer.2018.12.058

[10] S. Al-Jubouri, "Oily Water Treatment Using Ceramic Membrane," *Journal of Engineering*, vol. 17, no. 2, Apr. 2011, https://doi.org/10.31026/j.eng.2011.02.05

[11] H. R. Amedi and M. Aghajani, "Economic Estimation of Various Membranes and Distillation for Propylene and Propane Separation," *Industrial & Engineering Chemistry Research*, vol. 57, no. 12, pp. 4366–4376, Mar. 2018, https://doi.org/10.1021/acs.iecr.7b04169

[12] M. S. Shalaby, H. Abdallah, R. Wilken, A. M. Shaban, W. Abbas, G. Sołowski, and I. Sotnyk, "Economic assessment for TFC-RO membranes production for water desalination," *Chemical Engineering Science*, vol. 288, Apr. 2024, https://doi.org/10.1016/j.ces.2024.119805

[13] Y. Dong, H. Wu, F. Yang, and S. Gray, "Cost and efficiency perspectives of ceramic membranes for water treatment," *Water Research*, vol. 220, Jul. 2022, https://doi.org/10.1016/j.watres.2022.118629

[14] T. Gao, K. Xiao, J. Zhang, X. Zhang, X. Wang, S. Liang, J. Sun, F. Meng, and X. Huang, "Cost-benefit analysis and technical efficiency evaluation of full-scale membrane bioreactors for wastewater treatment using economic approaches," *Journal of Cleaner Production*, vol. 301, Jun. 2021, https://doi.org/10.1016/j.jclepro.2021.126984

[15] A. El-Gendi, H. Abdallah, and A. Amin, "Economic study for blend membrane production," *Bulletin of the National Research Centre*, vol. 45, no. 1, Dec. 2021, https://doi.org/10.1186/s42269-021-00584-0

[16] P. Yadav, N. Ismail, M. Essalhi, M. Tysklind, D. Athanassiadis, and N. Tavajohi, "Assessment of the environmental impact of polymeric membrane production," *Journal of Membrane Science*, vol. 622, Mar. 2021, https://doi.org/10.1016/j.memsci.2020.118987

[17] S. M. Al-Jubouri, S. Al-Batty, R. K. S. Al-Hamd, R. Sims, M. W. Hakami, and S. K. Manirul Haque, "Sustainable environment through using porous materials: A review on wastewater treatment," *Asia-Pacific Journal of Chemical Engineering*, vol. 18, issue 4, Jun. 2023, https://doi.org/10.1002/apj.2941

[18] H. Xu, K. Xiao, J. Yu, B. Huang, X. Wang, S. Liang, C. Wei, X. Wen, and X. Huang, "A simple method to identify the dominant fouling mechanisms during membrane filtration based on piecewise multiple linear regression," *Membranes*, vol. 10, no. 8, pp. 1–14, Aug. 2020, https://doi.org/10.3390/membranes10080171

[19] L. Hou, Z. Wang, and P. Song, "A precise combined complete blocking and cake filtration model for describing the flux variation in membrane filtration process with BSA solution," *Journal of Membrane Science*, vol. 542, pp. 186–194, 2017, https://doi.org/10.1016/j.memsci.2017.08.013

[20] S. A. Sadek and S. M. Al-Jubouri, "Structure and performance of polyvinylchloride microfiltration membranes improved by green silicon oxide nanoparticles for oil-in-water emulsion separation," *Materials Today Sustainability*, vol. 24, Dec. 2023, https://doi.org/10.1016/j.mtsust.2023.100600

[21] Z. Chen, G. Chen, H. Xie, Z. Xu, Y. Li, J. Wan, L. Liu, and H. Mao, "Photocatalytic antifouling properties of novel PVDF membranes improved by incorporation of SnO2-GO nanocomposite for water treatment," *Separation and Purification Technology*, vol. 259, Mar. 2021, https://doi.org/10.1016/j.seppur.2020.118184

[22] L. Marbelia, M. R. Bilad, A. Piassecka, P. S. Jishna, P. V. Naik, and I. F. J. Vankelecom, "Study of PVDF asymmetric membranes in a high-throughput membrane bioreactor (HT-MBR): Influence of phase inversion parameters and filtration performance," *Separation and Purification Technology*, vol. 162, pp. 6–13, Apr. 2016, https://doi.org/10.1016/j.seppur.2016.02.008
[23] E. O. Ezugbe and S. Rathilal, "Membrane technologies in wastewater treatment: A review," *Membranes*, vol. 10, issue 5, Apr. 2020, https://doi.org/10.3390/membranes10050089
[24] S. M. Abbas and S. M. Al-Jubouri, "High performance and antifouling zeolite@polyethersulfone/cellulose acetate asymmetric membrane for efficient separation of oily wastewater," *Journal of Environmental Chemical Engineering*, vol. 12, no. 3, Jun. 2024, https://doi.org/10.1016/j.jece.2024.112775
[25] H. Koonani and M. Amirinejad, "Combined three mechanisms models for membrane fouling during microfiltration," *Journal of Membrane Science and Research*, vol. 5, no. 4, pp. 274–282, 2019, https://doi.org/10.22079/jmsr.2019.95781.1224
[26] A. Y. Kirschner, Y. H. Cheng, D. R. Paul, R. W. Field, and B. D. Freeman, "Fouling mechanisms in constant flux crossflow ultrafiltration," *Journal of Membrane Science*, vol. 574, pp. 65–75, Mar. 2019, https://doi.org/10.1016/j.memsci.2018.12.001
[27] S. A. Sadek, S. M. Al-Jubouri, and S. Al-Batty, "Investigating the Fouling Models of the Microfiltration Mixed Matrix Membranes-Based Oxide Nanoparticles Applied for Oil-in-Water Emulsion Separation," *Iraqi Journal of Chemical and Petroleum Engineering*, vol. 25, no. 2, pp. 1–16, Jun. 2024, https://doi.org/10.31699/ijcpe.2024.2.1
[28] A. G. Saleem and S. M. Al-Jubouri, "Efficient Separation of Organic Dyes using Polyvinylidene Fluoride Polyethylene Glycol-Tin Oxide (PVDFPEG-SnO2) Nanoparticles Ultrafiltration Membrane," *Applied Science and Engineering Progress*, vol. 17, no. Special Issue, Aug. 2024, https://doi.org/10.14416/j.asep.2024.08.001
[29] M. C. Vincent Vela, S. Álvarez Blanco, J. Lora García, and E. Bergantiños Rodríguez, "Analysis of membrane pore blocking models adapted to crossflow ultrafiltration in the ultrafiltration of PEG," *Chemical Engineering Journal*, vol. 149, no. 1–3, pp. 232–241, Jul. 2009, https://doi.org/10.1016/j.cej.2008.10.027
[30] P. Kim, K. Park, H. G. Kim, and J. Kim, "Comparative analysis of fouling mechanisms of ceramic and polymeric micro-filtration membrane for algae harvesting," *Desalination and Water Treatment*, vol. 173, pp. 12–20, Jan. 2020, https://doi.org/10.5004/dwt.2020.24697
[31] S. Emani, R. Uppaluri, and M. K. Purkait, "Cross flow microfiltration of oil-water emulsions using kaolin based low cost ceramic membranes," *Desalination*, vol. 341, no. 1, pp. 61–71, May 2014, https://doi.org/10.1016/j.desal.2014.02.030

تحديد آلية التلوث المسيطرة باستخدام معادلات Hermia وحساب كلفة تصنيع أغشية البولي فينيلدين فلوريد فائقة الترشيح المعدلة

عبدالله غانم سليم [١]، سما محمد الجبوري [٢، *]، سرحان البطي [٣]، محمد والي حكمي [٣]

١ قسم الهندسة الكيميائية والبتروكيميائية، كلية الهندسة، جامعة الانبار، الانبار، العراق
٢ قسم الهندسة الكيمياوية، كلية الهندسة، جامعة بغداد، بغداد، العراق
٣ قسم تكنولوجيا الهندسة الكيميائية والعمليات، كلية الجبيل الصناعية، مدينة جبيل الصناعية، المملكة العربية السعودية

الخلاصة

تلوث الغشاء يعتبر المشكلة الرئيسية التي تحد من استخدام تكنولوجيا الأغشية. هذا العمل يركز على استخدام معادلات Hermia لتحديد آلية التلوث المسيطرة، والتي تتضمن انسداد المسام الجزئي، انسداد المسام الكلي، انسداد المسام القياسي، وتكوين الطبقة. كما أنه يتناول تقدير تكاليف التصنيع، والتي تشمل تكاليف مواد التحضير والطاقة المستهلكة أثناء عمليات التحضير والصب لأغشية البولي فينيلدين فلوريد/ البولي ايثيلين كلايكول (PVDF/PEG) والبولي فينيلدين فلوريد/ البولي ايثيلين كلايكول- أوكسيد القصدير النانوي ($PVDF/PEG-SnO_2$). نتائج معادلات Hermia تم تطبيقها على الدورات الأولى والثالثة والخامسة لعمليات ترشيح محلول صبغة رودامين ب (RhB). اعتماداً على معاملات المعادلات الخطية، فإن تلوث الغشاء يحدث في وقت واحد في جميع آليات التلوث. مع ذلك، فإن آلية التلوث المسيطرة هي تكوين الطبقة تليها انسداد المسام الجزئي. أثبت تحليل معاملات معادلات التلوث أن التلوث غير القابل للإزالة تجاوز التلوث القابل للإزالة عندما كانت قيمة معامل الارتباط (R^2) أعلى من ٠,٩٥، وهو ما يوضح الانخفاض المستمر في تدفق النفاذية لكلا الغشاءين المدروسين. أغشية البولي فينيلدين فلوريد المصنعة محلياً لم تتجاوز كلفة تصنيعها ٨٠ دولار لكل متر مربع. ايضاً، هذه الأغشية المصنعة تعتبر أرخص من أغشية البولي فينيلدين فلوريد النقية التي تصنعها شركة Guochukeji Technology (Xiamen).

الكلمات الدالة: غشاء البولي فينيلدين فلوريد، البولي ايثيلين كلايكول، أوكسيد القصدير، آليات التلوث، معادلات Hermia، حسابات الكلفة.